PHYSICAL REVIEW A **68**, 041801(R) (2003)

Low-light-level nonlinear optics with slow light

Danielle A. Braje,* Vlatko Balić, G. Y. Yin, and S. E. Harris
Edward L. Ginzton Laboratory, Stanford University, Stanford, California 94305, USA
(Received 25 April 2003; published 15 October 2003)

Electromagnetically induced transparency in an optically thick, cold medium creates a unique system where pulse-propagation velocities may be orders of magnitude less than c and optical nonlinearities become exceedingly large. As a result, nonlinear processes may be efficient at low-light levels. Using an atomic system with three, independent channels, we demonstrate a quantum interference switch where a laser pulse with an energy per area of ~ 23 photons per $\lambda^2/(2\pi)$ causes a $1/e$ absorption of a second pulse.

DOI: 10.1103/PhysRevA.68.041801 PACS number(s): 42.50.Gy, 32.80.Pj, 42.65.An

Interacting single photons, perhaps in an entangled state, are ideal candidates for applications in quantum information processing [1]. Because the strength of the interaction of single light quanta is typically weak, conventional nonlinear optics requires powerful laser beams focused tightly in nonlinear materials. When electromagnetically induced transparency (EIT) [2] is established in an optically thick medium with narrow resonance linewidths [3], a light pulse may experience exceedingly large nonlinearities, and nonlinear optical processes may become efficient at energy densities as low as a photon per atomic cross section [4]. Low-light-level nonlinear optics has been of recent interest in the context of resonant four-wave mixing [5], teleportation of atomic ensembles [6,7], production of correlated photon states [8], and quantum computation [9]. Ultimately, one may envision a waveguide geometry of an area $\sim\lambda^2/(2\pi)$ where a photon interacts with another photon by shifting its phase, by causing it to be absorbed, or by generating a third photon. Because the peak power of an individual photon may be varied by changing its bandwidth, the figure of merit for low-light-level nonlinear optical processes, as used here, is energy per area rather than power per area.

This paper focuses on an EIT-based, two-photon absorptive process suggested by Harris and Yamamoto [10] and observed by Zhu and co-workers [11]. Conceptually, this effect is the absorptive analog of the giant Kerr effect [12]. We report the demonstration of switching in an optically thick regime where a pulse with energy per area of ~ 23 photons per $\lambda^2/(2\pi)$ causes a $1/e$ absorption of a second pulse.

The lower portion of Fig. 1 shows both the prototype (lower left) and actual (lower right) atomic system used in the experiment. The coupling laser, tuned to the $|2\rangle \rightarrow |3\rangle$ transition with Rabi frequency $\Omega_c \equiv \mu_{23}E/\hbar$, creates a quantum interference which cancels the absorption and dispersion of the probe laser. Consequently, a probe laser of angular frequency ω_p has a slow group velocity and no absorption in the EIT medium [2]. The magnitude of the coupling laser and the optical depth of the medium determine both the allowable, EIT bandwidth and the group velocity of the probe beam. When a switching laser of angular frequency ω_s is applied, a second path is opened and simultaneous absorption of a probe and switching photon occurs.

In the actual atomic system, the three m_F states of the $5S_{1/2}(F=1)$ ground level are populated. With the polarizations as depicted in Fig. 1, there are three, parallel and independent channels, each of which contributes to the total susceptibility.

In the following paragraphs, we compare the experimental results with calculated quantities. The calculation includes dephasing and extends the results of Harris and Yamamoto [10] to the three, parallel channels of Fig. 1. We take the magnitude of the probe-laser Rabi frequency $|\Omega_p^{(i)}|$ to be sufficiently small as compared to the coupling laser Rabi frequency $|\Omega_c^{(i)}|$ so that the atomic population remains almost completely in the level $|1\rangle$. The susceptibility at the probe frequency of the multistate system is

$$\chi = \sum_{i=1}^{3} \frac{\mathcal{N}^{(i)}|\mu_{13}^{(i)}|^2}{\hbar\epsilon_0} \times \left[\frac{|\Omega_s^{(i)}|^2 - 4\Delta\tilde{\omega}_s\Delta\tilde{\omega}_c}{4\Delta\tilde{\omega}_p\Delta\tilde{\omega}_c\Delta\tilde{\omega}_s - |\Omega_c^{(i)}|^2\Delta\tilde{\omega}_s - |\Omega_s^{(i)}|^2\Delta\tilde{\omega}_p}\right]. \quad (1)$$

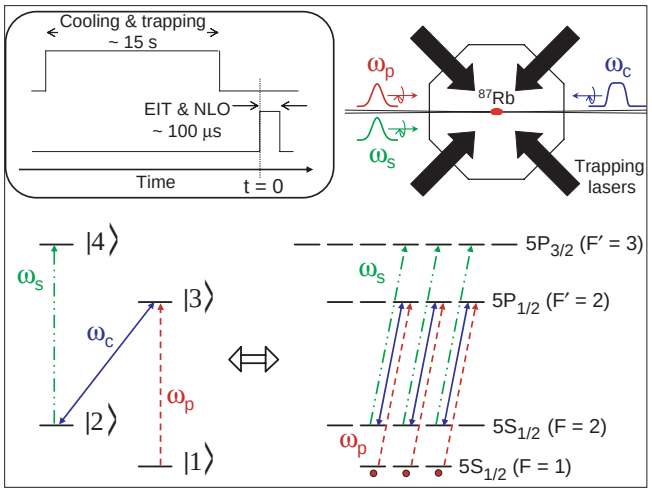

FIG. 1. (Color online) The experiment is performed in a 100-μs window 50 μs after shutting off the magnetic field and trapping lasers. The upper right corner depicts the laser beam orientations and polarizations. The lower left shows the prototype, four-level system; the lower right is the actual ^{87}Rb system used in the experiment.

*Electronic address: brajemanuszak@stanford.edu

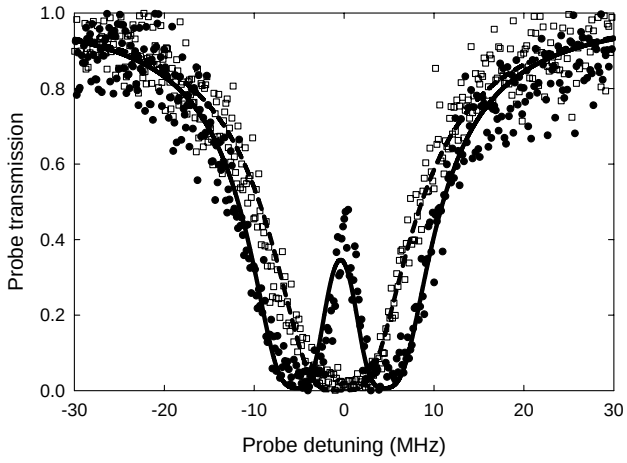

FIG. 2. Probe-laser transmission in the presence (●) and absence (□) of the coupling laser. Experimental parameters $N\sigma_{13}L=7.6$, $\Omega_c^{(1)}=\Omega_c^{(2)}=1.9\Gamma_3$, $\Omega_c^{(3)}=1.5\Gamma_3$, and $\gamma_{12}=0.2\Gamma_3$ are determined from a simultaneous, least-squares fit of absorption (dashed line) and EIT (solid line) data using Eq. (1).

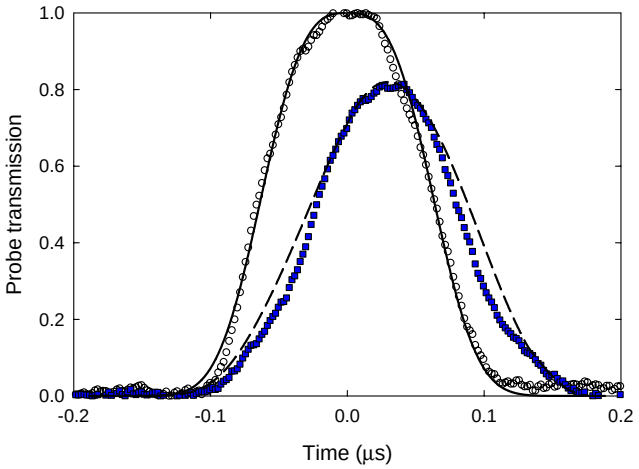

FIG. 3. Pulse delay. The reference pulse (○) is obtained without the presence of atoms. The EIT pulse (■) is delayed by 30 ns in a 0.8-mm atom cloud with a corresponding group velocity of $\sim c/10^4$. The solid line represents the experimental, Gaussian-like reference pulse. The dashed line shows the pulse shape and delay predicted by a theoretical model under the experimental conditions of $\Omega_c^{(1)}=\Omega_c^{(2)}=3.2\Gamma_3$, $\Omega_c^{(3)}=2.6\Gamma_3$, $\gamma_{12}=0.15\Gamma_3$, and $N\sigma_{13}L=6.5$.

Here, $\mu_{13}^{(i)}$ and $\mathcal{N}^{(i)}$ are the matrix element and density for the ith channel where $i=1,2,3$ corresponds to the states $m_F=-1,0,1$ of level $5S_{1/2}(F=1)$. The complex detunings are the same for each channel: $\Delta\tilde{\omega}_p=\omega_p-(\omega_3-\omega_1)+j\gamma_{13}$, $\Delta\tilde{\omega}_c=(\omega_p-\omega_c)-(\omega_2-\omega_1)+j\gamma_{12}$, $\Delta\tilde{\omega}_s=(\omega_p-\omega_c+\omega_s)-(\omega_4-\omega_1)+j\gamma_{24}$, where γ_{jk} are the respective dephasing rates. The imaginary and real parts of the propagation constant of the slowly moving probe beam give the E-field loss and phase shift per unit length of the envelope relative to vacuum: $\alpha=-\omega_p/(2c)\mathrm{Im}[\chi(\omega_p)]$ and $\beta=\omega_p/(2c)\mathrm{Re}[\chi(\omega_p)]$. The inverse group velocity of the probe relative to the freely propagating switching laser is $1/V_g=\partial\beta(\omega_p)/\partial\omega_p$.

Although certain aspects of EIT (such as slow and stopped light [13]) have been demonstrated successfully in room-temperature atomic samples, nonlinear optical effects at very low energies require cold atoms. For example, if this experiment were performed with copropagating, collimated laser beams as required for Doppler-free EIT at room temperature, the necessary energy density for switching would be increased by the Doppler linewidth over the natural linewidth of the switching transition (a factor of ~ 100). Our experiment is performed in a gas of cold ^{87}Rb atoms produced using a dark magneto-optical trap (MOT) [14]. A Ti:sapphire laser, which is locked 20 MHz below the $5S_{1/2}(F=2)\rightarrow 5P_{3/2}(F'=3)$ transition, supplies three, perpendicular, retroreflected, trapping beams. These beams have a $1/e$ diameter of 2 cm and a power in each beam of 65 mW. An extended-cavity, diode laser (ECDL) locked to the $5S_{1/2}(F=1)\rightarrow 5P_{3/2}(F'=2)$ transition acts as a repumping laser by recycling atoms from the $5S_{1/2}(F=1)$ level. Throughout the experiment, we maintain a Rb vapor pressure of $\sim 10^{-9}$ torr in a ten-port, stainless-steel vacuum chamber. The atoms are loaded into the MOT with a quadrupole magnetic-field gradient of 6 G/cm for 15 s. Three pairs of Helmholtz coils zero the background magnetic field. In order to compress the cloud, the magnetic-field gradient is ramped to 20 G/cm, and the trapping laser is detuned 50 MHz below resonance for 30 ms. By reducing the repumping intensity for 700 μs after initial compression, the atoms are shelved into the dark ($F=1$) ground level. The resulting atom cloud is 0.8 mm in diameter with measured atom number of $\sim 10^8$ atoms [15]. The experiment is performed in a 100-μs window, which starts 50 μs after shutting off the trapping beams and quadrupole fields at $t=0$ in Fig. 1. This cooling, trapping, and data-collection process is cycled at 0.05 Hz.

The coupling ECDL, with linewidth less than 300 kHz, is phase and frequency locked [16] on the D1 line to a reference ECDL (which is frequency stabilized to a saturated-absorption ^{85}Rb line). The probe laser is generated from the coupling laser by double passing through a 3.4-GHz acousto-optic modulator (AOM) which minimizes two-photon jitter. The switching laser is frequency stabilized in the same manner as the coupling laser on the D2 line of Rb. The shaping and timing of the probe, coupling, and switching lasers are controlled by separate AOMs. The probe and switching lasers are spatially filtered through the same single-mode, optical fiber. Their centers overlap within 10 μm, and each beam has a Gaussian profile with $1/e$ diameter of 212 μm in the atom cloud. The ~ 10 nW probe laser is detected on a photomultiplier tube with a 1.5-nm-wide bandpass filter. Probe transmission data are obtained using a 100-μs pulse with a calibrated, nearly linear chirp of 0.6 MHz/μs averaged over ten atom clouds.

The experimental probe transmission in the absence of the coupling laser is shown by the boxed points in Fig. 2. A least-squares fit (dashed curve) taking into account all channels allows the determination of the total $NL=(9.0\pm 0.2)\times 10^9$ atoms/cm^2. With the ith channel, state to state, atomic absorption cross section defined as $\sigma_{13}^{(i)}\equiv\omega_{13}|\mu_{13}^{(i)}|^2/(c\epsilon_0\hbar\gamma_{13})$, the absorption of the probe beam is

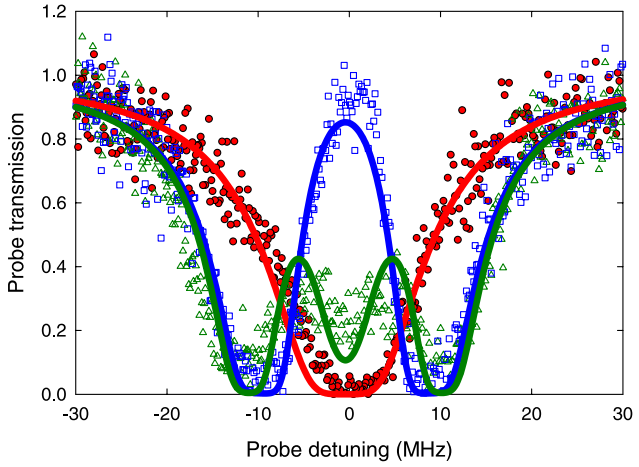

FIG. 4. (Color online) Probe transmission for absorption (●), EIT (□), and switching (△) averaged over ten atom clouds. Data are taken by detuning the probe laser while switching and coupling lasers are on resonance. The solid lines represent a simultaneous, least-squares fit to all three curves where $N\sigma_{13}L=8.9$, $\gamma_{12}=0.1\Gamma_3$, $\Omega_c^{(1)}=\Omega_c^{(2)}=3.6\Gamma_3$, $\Omega_c^{(3)}=2.9\Gamma_3$, $\Omega_s^{(1)}=1.1\Gamma_3$, $\Omega_s^{(2)}=1.5\Gamma_3$, and $\Omega_s^{(3)}=2.0\Gamma_3$.

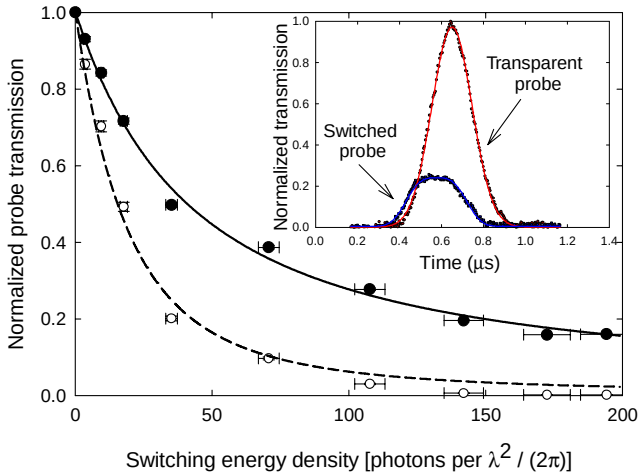

FIG. 5. (Color online) Probe transmission [raw data (●) and data corrected for Gaussian spatial profile (○)] is normalized to EIT transmission of 60%. All lasers are on resonance, $\Omega_c^{(1)}=\Omega_c^{(2)}=2.0\Gamma_3$, $\Omega_c^{(3)}=1.7\Gamma_3$, $N\sigma_{13}L=7.5$, and $\gamma_{12}=0.15\Gamma_3$. Inset: Probe pulse (raw data) with and without the switching laser applied.

$\exp(-N\sigma_{13}L)$, where $\sigma_{13}\equiv\frac{1}{3}\Sigma_{i=1}^{3}\sigma_{13}^{(i)}$ is the channel-averaged cross section and L is the length of the atomic sample. The optical depth in Fig. 2 is $N\sigma_{13}L=7.6\pm0.2$.

With the coupling laser applied, we obtain a probe transmission whose peak value is dependent on the intensity of the coupling laser. In the ideal case when there is no dephasing of the $|1\rangle\rightarrow|2\rangle$ transition, $|\Omega_c|$ may be made arbitrarily small without loss of transmission. When there is a nonzero dephasing rate, $\gamma_{12}\neq0$, the probe laser experiences some absorption. For reasonable transmission, the minimum $|\Omega_c|$ must be much greater than γ_{12}. A least-squares fit of the EIT profile determines the coupling laser power per area and dephasing rate as $P_c/A=(42.4\pm1.7)$ mW/cm^2 and $\gamma_{12}=(0.22\pm0.02)\Gamma_3$, respectively. The Rabi frequency $\Omega_c^{(i)}$ of each channel is $\Omega_c^{(1)}=\Omega_c^{(2)}=1.9\Gamma_3$ and $\Omega_c^{(3)}=1.5\Gamma_3$, where $\Gamma_3=2\pi\times5.7\times10^6$ s^{-1} is the Einstein A coefficient of the $5P_{1/2}$ level. The solid line in Fig. 2 shows probe transmission under the above conditions. By doubling the coupling laser Rabi frequency, we observe on-resonance probe transmission greater than 95% as shown in Fig. 4.

Associated with the narrow, EIT, transmission window is a steep, dispersive profile, and a correspondingly small group velocity. Figure 3 shows a probe pulse (filled boxes) with a group velocity of $\sim c/10^4$ delayed by 30 ns from the reference pulse (circles) in our experiment. The theoretical curve (dashed line) is obtained by numerically solving the slowly varying envelope equations simultaneously with the density-matrix equations for all relevant, hyperfine states. The numerical curve is absolute with no free parameters.

By adding a third laser with frequency ω_s tuned to the $|2\rangle\rightarrow|4\rangle$ transition of the cold-atom, ^{87}Rb system, efficient two-photon absorption is observed. Figure 4 shows absorption, EIT, and switching as a function of the detuning of the probe laser while switching and coupling lasers are on-resonance. The large coupling laser Rabi frequency dominates over the small dephasing rate allowing nearly 100% transparency. The switching data (shown as triangles in Fig. 4) follow the characteristic shape predicted by Eq. (1). The solid lines represent a least-squares fit of absorption, EIT, and switching using the three-channel susceptibility.

We next examine two-photon absorption in a pulsed regime. Figure 5 shows probe transmission normalized to EIT transmission (raw data ●) as a function of the energy per area of the switching laser pulse. Each data point is obtained by averaging a train of 50 pulses in one cloud event. These pulses have a temporal length of 350 ns, and they are repeated every 1 μs. During this data-collection period, there is no observable change in transparency. In order to eliminate the effect of atom number fluctuations in each atom cloud, the pulse trains are averaged over ten clouds. The data which are corrected for the spatial transverse Gaussian profile of the switching beam (○) are shown in the same figure. (These data could have been obtained by using a small pinhole, about 10 μm in diameter, to read the peak of the Gaussian beams.) From this plot we infer $1/e$ switching at $\sim$23 photons per $\lambda^2/(2\pi)$.

For the prototype system of Fig. 1 under the assumptions that $N\sigma L\gg1$ for effective switching and $\gamma_{12}\ll|\Omega_c|$, the switching power per area $(P_s/A)_{crit}$ for $1/e$ switching from normalized probe transmission is

$$\frac{1}{\hbar\omega_s}\left(\frac{P_s}{A}\right)_{crit}=\frac{1}{(N\sigma_{13}L)\sigma_{24}}\left(\frac{|\Omega_c|^2}{2\gamma_{13}}+4\gamma_{12}\right). \qquad (2)$$

In the parallel-channel system, differing matrix elements prevent Eq. (2) from becoming a simple sum over the three channels as in the susceptibility; however, Eq. (2) may be used to estimate the required switching power. Using the experimental parameters $N\sigma_{13}L$ and average $|\Omega_c|$, $(P_s/A)_{crit}=4.3$ mW/cm^2 or 5.4 photons per $\lambda^2/(2\pi)$. This estimate is in reasonable agreement with experimental results.

We have considered the case where the probe beam propagates very slowly and the switching laser propagates at the speed of light. Once the probe pulse is compressed inside the medium, a decrease of the coupling laser power both increases the nonlinearity and decreases the interaction length by further compressing the pulse. Here the energy density limit for 1/e absorption, independent of $|\Omega_c|^2$, is about one photon per atomic cross section [4]. In order to increase our switching efficiency to reach this energy density, $|\Omega_c|$ must be decreased; however, the dephasing rate of the medium, γ_{12}, ultimately bounds the coupling laser Rabi frequency. Our non-negligible, effective dephasing may result from the finite temperature of the atomic sample as well as from state mixing and Zeeman shifts due to residual, transient, and inhomogeneous magnetic fields. The anomalous dephasing rate could be reduced in a dipole trap. Overcoming this dephasing rate will allow the implementation of ideas for simultaneous slowing of both probe and switching pulses [17]. In this case, the required number of photons per area for a nonlinear optical process may be well less than unity.

The dephasing rate imposes a limit not only on nonlinear optics, but also on EIT-associated phenomena such as slow group velocity and pulse compression. In ideal stopped-light experiments, which are of significant interest for quantum information storage and processing, the probe pulse compresses entirely in the medium. One can show that in the three-state, EIT system, the maximum number of Gaussian pulses that can be stacked in a medium is given by

$$\mathbb{N}_{\max}=\frac{N\sigma_{13}L}{2\sqrt{2}\,\ln 2}\left(\frac{1}{2N\sigma_{13}L}-\frac{2\gamma_{12}\gamma_{13}}{|\Omega_c|^2}\right)^{1/2}. \tag{3}$$

Here we have assumed that $\gamma_{12}\gamma_{13}\ll|\Omega_c|^2$ and that the pulse bandwidth $\Delta\omega_p$ is limited by the EIT bandwidth where $\Delta\omega_p\ll|\Omega_c|$. At large optical depths, the dephasing is the dominant limit for storable pulses. In the present experiment, we demonstrate less than one storable pulse.

The combination of EIT and cold atoms enables nonlinear optical processes which can be used to study interactions at very low energies. This paper demonstrates two-photon switching in a three-parallel-channel system at an energy per area of ~ 23 photons per $\lambda^2/(2\pi)$. The three-channel system described here may be immediately useful for controlled storage of photons in a (processible) three-component superposition state [7].

We acknowledge helpful discussions with Vladan Vuletić, Jamie Kerman, and Cheng Chin on atom cooling and trapping. This work was supported by the U.S. Air Force Office of Scientific Research, the U.S. Army Research Office, the U.S. Office of Naval Research, Multidisciplinary Research Initiative Program, and the Fannie and John Hertz Foundation (D.A.B.).

[1] M.D. Lukin and A. Imamoğlu, Nature (London) **413**, 273 (2001).
[2] S.E. Harris, Phys. Today **50**(7), 36 (1997); J.P. Marangos, J. Mod. Opt. **45**, 471 (1998); Robert W. Boyd, *Progress In Optics* (Elsevier, Amsterdam, 2002), Vol. 43, p. 497.
[3] L.V. Hau, S.E. Harris, Z. Dutton, and C.H. Behroozi, Nature (London) **397**, 594 (1999).
[4] S.E. Harris and L.V. Hau, Phys. Rev. Lett. **82**, 4611 (1999).
[5] Mattias T. Johnsson and Michael Fleischhauer, Phys. Rev. A **66**, 043808 (2002); A.S. Zibrov, M.D. Lukin, and M.O. Scully, Phys. Rev. Lett. **83**, 4049 (1999).
[6] A. Furusawa *et al.*, Science **282**, 706 (1998).
[7] L.-M. Duan *et al.*, Nature (London) **414**, 413 (2001).
[8] C.H. van der Wal *et al.*, Science **301**, 196 (2003); A. Kuzmich *et al.*, Nature (London) **423**, 731 (2003).
[9] Carlo Ottaviani *et al.*, Phys. Rev. Lett. **90**, 197902 (2003); M.O. Scully and M.S. Zubiary, *Quantum Optics* (Cambridge University Press, Cambridge, 1997).
[10] S.E. Harris and Y. Yamamoto, Phys. Rev. Lett. **81**, 3611 (1998).
[11] Min Yan, Edward G. Rickey, and Yifu Zhu, Phys. Rev. A **64**, 041801(R) (2001).
[12] H. Schmidt and A. Imamoğlu, Opt. Lett. **21**, 1936 (1996).
[13] Michael Kash *et al.*, Phys. Rev. Lett. **82**, 5229 (1999); Phillips *et al.*, *ibid.* **86**, 783 (2001).
[14] Wolfgang Ketterle *et al.*, Phys. Rev. Lett. **70**, 2253 (1993); C.G. Townsend *et al.*, Phys. Rev. A **53**, 1702 (1996).
[15] Ying-Cheng Chen *et al.*, Phys. Rev. A **64**, 031401(R) (2001).
[16] M. Prevedelli, T. Freegarde, and T.W. Hänsch, Appl. Phys. B: Lasers Opt. **60**, S241 (1995).
[17] M.D. Lukin and A. Imamoğlu, Phys. Rev. Lett. **84**, 1419 (2000); David Petrosyan and Gershon Kurizki, Phys. Rev. A **65**, 033833 (2002).